Article

Single Molecule Spectroscopic Investigation on Conformational Heterogeneity of Directly Linked Zinc(II) Porphyrin Arrays

Mira Park, Sung Cho, Zin Seok Yoon, Naoki Aratani, Atsuhiro Osuka, and Dongho Kim

J. Am. Chem. Soc., **2005**, 127 (43), 15201-15206• DOI: 10.1021/ja0544861 • Publication Date (Web): 07 October 2005

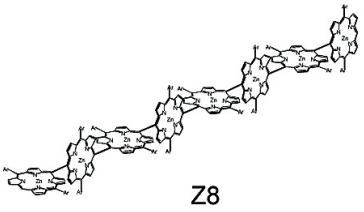

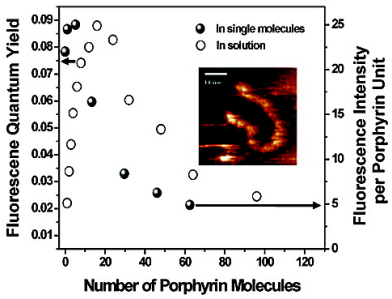

More About This Article

Additional resources and features associated with this article are available within the HTML version:

- Supporting Information
- Links to the 5 articles that cite this article, as of the time of this article download
- Access to high resolution figures
- Links to articles and content related to this article
- Copyright permission to reproduce figures and/or text from this article

View the Full Text HTML

J|A|C|S
ARTICLES
Published on Web 10/07/2005

Single Molecule Spectroscopic Investigation on Conformational Heterogeneity of Directly Linked Zinc(II) Porphyrin Arrays

Mira Park,[†] Sung Cho,[†] Zin Seok Yoon,[†] Naoki Aratani,[‡] Atsuhiro Osuka,*[,‡] and Dongho Kim*[,†]

Contribution from the Center for Ultrafast Optical Characteristics Control and Department of Chemistry, Yonsei University, Seoul 120-749, Korea, Department of Chemistry, Graduate School of Science, Kyoto University, and Core Research for Evolutional Science and Technology (CREST), Japan Science and Technology Agency (JST), Sakyo-ku, Kyoto 606-8502, Japan

Received July 7, 2005; E-mail: dongho@yonsei.ac.kr; osuka@kuchem.kyoto-u.ac.jp

Abstract: We have comparatively investigated the photophysical properties of a series of *meso*−*meso* directly linked orthogonal porphyrin arrays (**Z*n***, ***n*** = **1**, **2**, **3**, **4**, **6**, **8**, **9**, **12**, **16**, **32**, **48**, **64**, and **96**) by ensemble average and single molecule fluorescence spectroscopy. In single molecule fluorescence study, we have recorded the fluorescence intensity trajectories of **Z*n*** arrays as the number of porphyrin molecules in the array increases. Up to **Z8** in porphyrin arrays, each single array exhibits multiple stepwise photobleaching behaviors in fluorescence intensity trajectories, indicating that each porphyrin unit in the array acts as an individual fluorescent unit due to a maintenance of linear rigid structure of the array. On the other hand, porphyrin arrays longer than **Z8** such as **Z16**, **Z32**, **Z48**, and **Z64** show complicated photobleaching behaviors in fluorescence intensity trajectories. The origin of complex photobleaching behaviors is believed to be increasing nonradiative decay channels contributed by the enhanced structural nonlinearity in longer arrays. The fluorescence measurements of **Z*n*** arrays on single molecule level show a mismatch in the maximum fluorescence intensity level as compared to the solution measurements, which is attributable to the difference in local environment surrounding the porphyrin array. In this work, we have demonstrated the presence of conformational heterogeneity in longer porphyrin arrays by analyzing average survival times and fluorescence spectra of single arrays as the number of porphyrin molecules in the array increases. We believe that the fluorescence properties of porphyrin arrays on single molecule level will provide a platform for further applications as molecular photonic wires.

Introduction

Energy transfer and migration in natural light harvesting systems are highly efficient despite involving complex structures with many chlorophyll molecules. Because of the complexity of naturally occurring light harvesting processes, great efforts have been devoted to the synthesis and characterization of artificial systems that can elucidate or mimic key mechanisms of energy migration in natural light harvesting systems.[1−4] As a consequence, the artificial systems have been utilized for various applications such as molecular photonic and electronic devices.[5,6]

In recent years, porphyrin arrays have been considered as ideal models of mimicking the natural light harvesting systems because the structure of porphyrin is similar to their constituent units such as chlorophyll and bacteriochlorophyll. Therefore, the challenge of creating artificial mimicries of these complexes has stimulated the development of various multi-porphyrin arrays.[7−16]

Some requirements such as long array length, short linker, and well-defined structure should be considered for the development of new-types of porphyrin arrays, which exhibit much enhanced light energy transfer efficiency as compared to the existing synthesized porphyrin arrays. Long array length is essential for the linkage between energy donor and acceptor

[†] Yonsei University.
[‡] Kyoto University and CREST.

(1) Prathanpan, S.; Johnson, T. E.; Lindsey, J. S. *J. Am. Chem. Soc.* **1993**, *115*, 7519.
(2) Seth, J.; Palaniappan, V.; Johnson, T. E.; Prathapan, S.; Lindsey, J. S.; Bocian, D. F. *J. Am. Chem. Soc.* **1994**, *116*, 10578.
(3) McDermott, G. M.; Prince, S. M.; Freer, A. A.; Hawthonthwaite-Lawless, A. M.; Papiz, Z.; Cogdell, R. J.; Isaacs, N. W. *Nature* **1995**, *374*, 517.
(4) Pullerits, T.; Sundström, V. *Acc. Chem. Res.* **1996**, *29*, 381.
(5) Wagner, R. W.; Lindsey, J. S. *J. Am. Chem. Soc.* **1994**, *116*, 9759.
(6) Wagner, R. W.; Lindsey, J. S.; Seth, J.; Palaniappan, V.; Bocian, D. F. *J. Am. Chem. Soc.* **1996**, *118*, 3996.
(7) Aratani, N.; Osuka, A.; Kim, Y. H.; Jeong, D. H.; Kim, D. *Angew. Chem., Int. Ed.* **2000**, *39*, 1458.
(8) Kim, Y. H.; Jeong, D. H.; Kim, D.; Jeoung, S. C.; Cho, H. S.; Kim, S. K.; Aratani, N.; Osuka, A. *J. Am. Chem. Soc.* **2001**, *123*, 76.
(9) Cho, H. S.; Jeong, D. H.; Cho, S.; Kim, D.; Matsuzaki, Y.; Tanaka, K.; Tsuda, A.; Osuka, A. *J. Am. Chem. Soc.* **2002**, *124*, 14642.
(10) Kim, D.; Osuka, A. *J. Phys. Chem. A* **2003**, *107*, 8791.
(11) Kim, D.; Osuka, A. *Acc. Chem. Res.* **2004**, *97*, 735.
(12) Aratani, N.; Cho, H. S.; Ahn, T. K.; Cho, S.; Kim, D.; Sumi, H.; Osuka, A. *J. Am. Chem. Soc.* **2003**, *125*, 9668.
(13) Strachan, J. P.; Gentemann, S.; Seth, J.; Kalsbeck, W. A.; Linsey, J. S.; Holten, D.; Bocian, D. F. *J. Am. Chem. Soc.* **1997**, *119*, 11191.
(14) Lammi, R. K.; Ambrolse, A.; Balasubramanian, T.; Wagner, R. W.; Bocian, D. F.; Holten, D.; Lindsey, J. S. *J. Am. Chem. Soc.* **2000**, *122*, 7579.
(15) Tsuda, A.; Osuka, A. *Science* **2001**, *293*, 79.
(16) Richeter, S.; Jeandon, C.; Ruppert, R.; Callot, H. J. *Chem. Commun.* **2001**, 91.

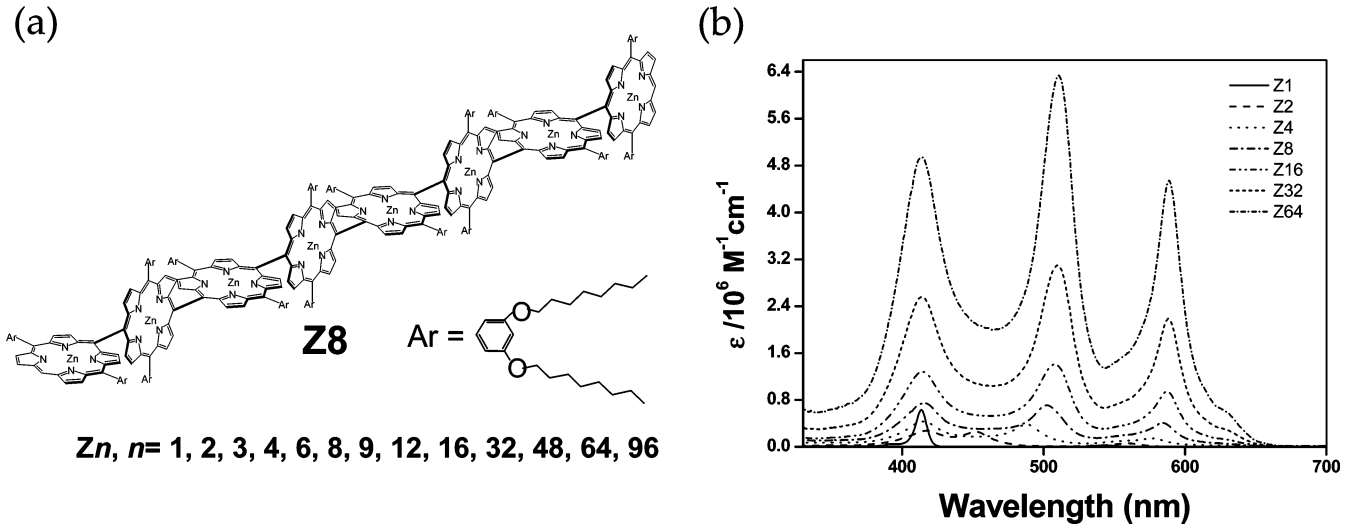

Figure 1. Molecular structure of representative *meso*−*meso* directly linked orthogonal Zn(II) porphyrin array (**Z8**) and molar extinction coefficient spectra of a series of ***Zn*** arrays up to 64-mer.

over a long distance. Also, short linker and well-defined structure are prerequisite for efficient energy transfer to be void of energy sink, because strong dipole couplings between adjacent units in the array are a controlling factor in efficient energy migration along the array.

In these respects, the *meso*−*meso* directly linked orthogonal porphyrin arrays (see Figure 1a) are considered as an ideal candidate for a highly efficient energy transfer system. Because they do not have any linkers, orthogonal architecture allows for linearity due to a large steric hindrance between neighboring porphyrin molecules. From previous studies, the radiative coherent length (the ratio of the radiative decay rates in the arrays to that of monomer) in these porphyrin arrays was estimated to be about four porphyrin molecules experimentally and theoretically.[7−12] The radiative coherence length is very important in understanding the energy transfer efficiency and the related excitation energy flow because excitation is delocalized over several molecules in the porphyrin array. From this result, this porphyrin array can be considered to exhibit efficient energy migration. Despite the expected linear rigid structure of the orthogonally directly linked porphyrin arrays, the evaluated radiative coherent length of four porphyrin units is considered to be relatively short. In other words, while each porphyrin constituent in the array acts as an individual absorbing chromophore as evidenced by a linear summation behavior of molecular extinction coefficients (Figure 1b), the fluorescence quantum yield of the array shows a saturation behavior as the number of porphyrin moieties in the array increases. This feature can be regarded to arise from conformational heterogeneity especially in long arrays contributed by the summation of dihedral and tilting angles between adjacent porphyrins. Conformational heterogeneity due to geometrical flexibilities can act as nonradiative quenching sites in excitation energy migration processes, and the overall photophyscial properties can be altered by this feature. Therefore, it is quite relevant to understand the singlet excited-state behaviors of Zn(II) porphyrin arrays at single molecule level to explore the relationship between the ensemble average properties and the summation of each individual property in different local environments.

In this study, we have investigated conformational heterogeneities for the orthogonal porphyrin arrays by both ensemble and single molecule spectroscopy as the number of porphyrin molecules in the array increases. Single molecule fluorescence measurements have provided detailed information related to the conformational heterogeneity of each porphyrin array. Thus, it can be expected that our study will be a benefit to the development of single molecular devices for future applications as molecular photonic wires.

Experimental Section

Instrumentation. A laser scanning confocal microscope (LSCM) system based on an inverted type optical microscope was used for fluorescence detection of single molecule. The sample scanning was achieved by using an $x-y$ scanning sample stage consisting of two electrostrictive actuators (AD-100, New Port) and a two-axis linear translator stage. The excitation laser beam at 543.5 nm from a He−Ne laser (25 LGR 193-230, Melles Griot) was delivered to the input port of the confocal microscope through a single-mode optical fiber. The laser beam from the fiber was filtered by a narrow-band interference filter (F10-546.1-4-1.00, CVI Laser Corp.), and then reflected up to the microscope objective lens (Plan-neofluar 100× oil immersion, Carl Zeiss) by using a dichroic beam splitter (565DCXR, Chroma). The laser beam was expanded to 10 mm in diameter before it impinged on the excitation filter to obtain higher optical resolution. When we recorded the fluorescence intensity of a single molecule at the focal point of objective lens with linear scanning, the intensity versus distance curve exhibited a beam diameter of 300 nm in fwhm with Gaussian fitting. Fluorescence of single molecules was collected by the same microscope objective lens and focused through a 150 mm focal length lens onto an APD detector in a single photon counting mode (SPCM-AQR-14-FC, EG&G, Perkin Elmer Optoelectronics, Norwalk, CT). Scattered light around the excitation wavelength was removed by placing a suitable filter between the objective lens and the focusing lens. The electrical pulses from the output of an APD detector were counted with a computer plug-in counter board (PCI 6602, National Instruments). Sample stage scanning and data acquisition were controlled by a personal computer based on the Visual Basic program. The fluorescence spectra were measured with a liquid nitrogen-cooled CCD camera (LN/CCD 512SB, Princeton Instruments) coupled to a 150 mm spectrograph (SpectroPro 150, Acton Research Corp.) in 10 s exposure time.

Sample Preparation and Steady-State Spectroscopic Measurements. The details on the synthesis of porphyrin arrays studied here

were documented in the relevant previous papers.[7,8,12,19−21] Steady-state absorption spectra were recorded by using a Shimadzu model 1601 UV spectrometer, and fluorescence measurements were made on a Hitachi model F-4500 spectrofluorometer at room temperature.

Samples for single molecule measurements were prepared by spin-coating a solution of Zn(II) porphyrin arrays ($\sim 10^{-10}$ M) in toluene containing 1 mg/mL polymethyl methacrylate (PMMA) on a cover glass. Polymethyl methacrylate (PMMA) (MW = 120 000) was purchased from Sigma-Aldrich Co. HPLC grade toluene (Merck) was used as solvent. Optical density of the dye solution was measured to determine the concentration. The solution was then successively diluted down to 10^{-10}. Films for single molecule fluorescence detection (Supporting Information 1) were prepared by spin coating (2000 rpm) the sample solution onto rigorously cleaned cover glasses or polymer films on cover glasses.

Results and Discussion

Ensemble Spectroscopy. Figure 1 shows the molecular structures of a series of *meso*−*meso* directly linked Zn(II) porphyrin arrays (**Z*n***, ***n* = 1**, **2**, **3**, **4**, **6**, **8**, **9**, **12**, **16**, **32**, **48**, **64**, and **96**) and their molar extinction coefficient spectra in tetrahydrofuran (THF).

As reported previously,[8,22−24] Zn(II) porphyrin monomer (**Z1**) displays characteristic Q- and B-absorption bands corresponding to the S_1 and S_2 states, and their *meso*−*meso* linked Zn(II) porphyrin arrays exhibit a large splitting of the B-bands mainly due to exciton-coupling. On the other hand, the Q-bands of **Z*n*** arrays show relatively much weaker splitting as well as a small red-shift, indicating a weak coupling of transition dipoles and a negligible π-conjugation, respectively, between adjacent porphyrin molecules in the array. As is illustrated in Figure 1b, as the porphyrin arrays become longer, the molar absorptivity shows a linear summation behavior. In other words, each porphyrin unit in the array acts as an independent light-absorbing unit. In contrast, the fluorescence quantum yields (Φ_f) of **Z*n*** arrays show a maximum value at **Z16** and decrease as the array becomes longer than **Z16** (Supporting Information 2). Such a feature can be explained by the fact that the increasing nonradiative decay channels due to the formation of nonlinear structures in longer porphyrin arrays decrease the fluorescence quantum yields (Supporting Information 2). The fluorescence decays of **Z*n*** arrays show a similar trend. The fluorescence decay is well fitted by a monoexponential function up to **Z16**, with $\tau = 2.4$ ns for **Z1**. On the other hand, the fluorescence decays start to show biexponential behavior as the array becomes longer than **Z16**. The decrease in fluorescence lifetimes of **Z*n*** as the array becomes longer is also consistent with the geometry changes in **Z*n***, because the structural heterogeneity is expected to act as nonradiative quenching sites in excitation energy migration processes.

Single Molecule Fluorescence Intensity Traces. The fluorescence quantum yields of **Z*n*** arrays observed on the basis of ensemble measurements were very low ($\Phi_f < 0.1$). Hence, it can be easily anticipated that it is difficult to observe photobleaching behaviors in fluorescence intensity trajectories of single molecules within a bin time shorter than 20 ms. Figure 2 shows the fluorescence intensity trajectories of **Z1**, **Z2**, and **Z3** single molecules embedded in a PMMA polymer matrix using 543.5 nm continuous wave excitation light. On/off behaviors as well as jumps in fluorescence intensity trajectories were clearly detected during the excitation.

About 53% of the investigated trajectories for **Z1** molecules show a single stepwise photobleaching, as can be expected for a single porphyrin unit. 38% of double stepwise fluorescence intensity levels were detected for **Z2** dimer. In this case, after one porphyrin unit is photobleached, the fluorescence intensity level of the other porphyrin unit drops to the background level. The triple stepwise photobleaching of **Z3** array was observed only in 12%. The fluorescence intensity trajectories of some molecules show multiple intensity levels in the photobleaching process such as a spectral jump due to the variations in local environment surrounding the molecule as well as the changes in emission polarization. The spectral jumps in the fluorescence intensity trajectories of some molecules obscure the number of photobleaching events in the stepwise photobleaching process. In addition, the fluorescence intensity trajectories especially in long arrays show less emissive levels than the number of porphyrin units in the array due to early photobleaching before recording the fluorescence intensity trajectories. The trajectories of **Z2** and **Z3** arrays show longer survival times as compared to those of **Z1** under identical excitation conditions. Multiple stepwise photobleaching behaviors detected in **Z2** and **Z3** arrays were similar to the previous results found for the single molecule with multichromophores.[25] Up to **Z8**, the typical fluorescence intensity trajectories show multiple stepwise behaviors, indicating that each porphyrin unit in the array acts as an individual absorbing and fluorescing chromophore due to the maintenance of linear conformation and the weak coupling between neighboring porphyrin moieties as was observed in the absorption spectra and fluorescence quantum yields in solution. Moreover, by comparing the photobleaching behaviors in the fluorescence intensity trajectories of **Z8**, **Z16**, and **Z32**, one can clearly see that in long arrays the fluorescence intensity trajectories show on/off behaviors such as reversible intensity jump. Figure 2f shows photobleaching behavior of the single **Z32** array, showing complex on/off behaviors with relatively large fluctuations as compared to stepwise behaviors in short arrays. The duration of off-states varies from 20 ms to hundreds of milliseconds. Because we have recorded the fluorescence intensity trajectories of porphyrin arrays in 20−30 ms/pixel binning time intervals, the contribution by the triplet states of porphyrin arrays to the dark states in the fluorescence intensity trajectories can be eliminated. Thus, the reason for the off-process of several tens of milliseconds in a single **Z32** array is different from that of the triplet off-process. At this point, it must be emphasized that in the **Z32** array nonlinear conformation affects the fluorescence properties of porphyrin units such as fluorescence traps or nonradiative decay channels, although the nature of the off-state is not fully understood. Hence, the geometrical distribution in the long arrays such as conformational heterogeneity can be

(17) Anderson, H. L. *Chem. Commun.* **1999**, 2323.
(18) Blake, I. M.; Rees, L. H.; Claridge, T. D. W.; Anderson, H. L. *Angew. Chem., Int. Ed.* **2000**, *39*, 1818.
(19) Osuka, A.; Shimidzu, H. *Angew. Chem., Int. Ed. Engl.* **1997**, *36*, 135.
(20) Nakano, A.; Yamazaki, T.; Nishimura, Y.; Yamazaki, I.; Osuka, A. *Chem.-Eur. J.* **2000**, *6*, 3254.
(21) Yoshida, N.; Aratani, N.; Osuka, A. *Chem. Commun.* **2000**, 197.
(22) Cho, H. S.; Song, N. W.; Kim, Y. H.; Jeoung, S. C.; Hahn, S.; Kim, D.; Kim, S. K.; Yoshida, N.; Osuka, A. *J. Phys. Chem. A* **2000**, *104*, 3287.
(23) Cho, H. S.; Jeong, D. H.; Yoon, M.-C.; Kim, Y.-R.; Kim, D.; Jeoung, S. C.; Kim, S. K.; Aratani, N.; Shinmori, H.; Osuka, A. *J. Phys. Chem. A* **2001**, *105*, 4200.
(24) Kim, Y. H.; Cho, H. S.; Kim, D.; Kim, S. K.; Yoshida, N.; Osuka, A. *Synth. Met.* **2001**, *117*, 183.
(25) Hofkens, J.; Maus, M.; Gensch, T.; Vosch, T.; Cotlet, M.; Köhn, F.; Herrmann, A.; Müllen, K.; De Schryver, F. C. *J. Am. Chem. Soc.* **2000**, *122*, 9278.

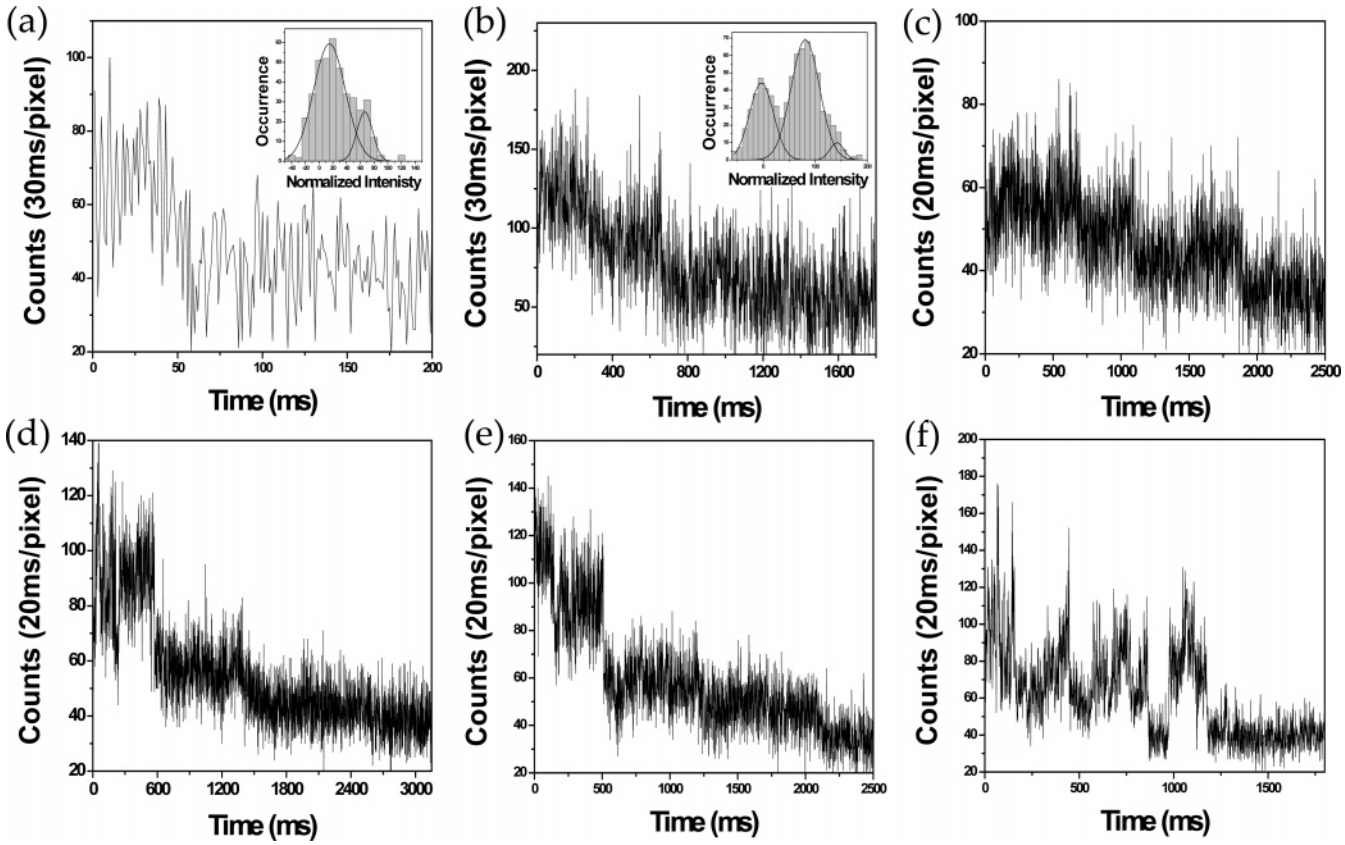

Figure 2. Fluorescence intensity trajectories of **Z1** (a), **Z2** (b), **Z3** (c), **Z8** (d), **Z16** (e), and **Z32** (f) arrays embedded in a PMMA polymer matrix at an average power of 1.5 μW and atmospheric condition. The inset represents the histogram of the occurrences of fluorescence intensity trajectories given in (a) and (b).

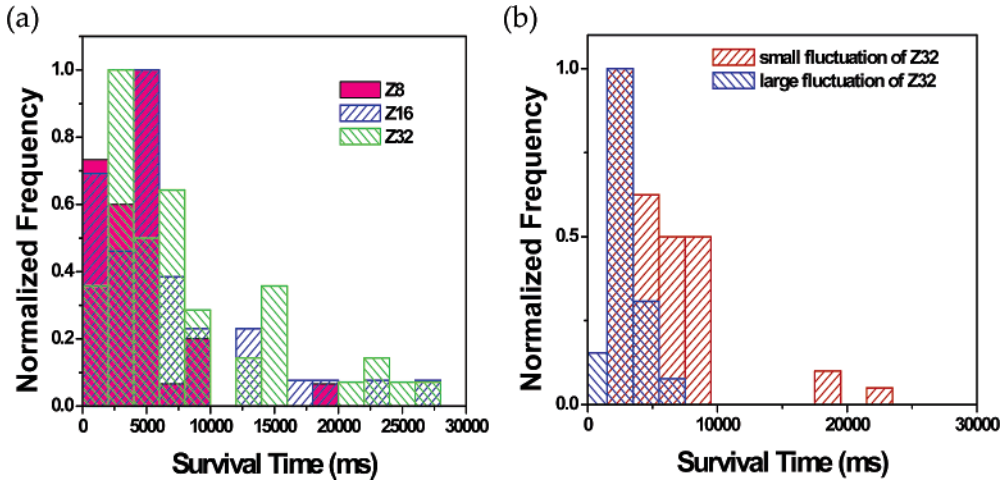

Figure 3. Distribution of the survival times of **Z8**, **Z16**, and **Z32** (a). Distribution of the survival times of **Z32** arrays with small and large fluctuations in fluorescence intensity trajectories (b).

expressed as transient behaviors with large fluctuations and nonstepwise fluorescence intensity trajectories.

Survival times correspond to the lowest levels in the fluorescence intensity trajectory before irreversible photobleaching of all porphyrin molecules in the array occurs. As is displayed in Figure 3, as the porphyrin array increases from **Z8** to **Z32**, the mean survival times in fluorescence intensity trajectories do not increase linearly, although there is a slight increase in the overall survival times. This feature suggests that the number of fluorescence trapping sites acting as nonradiative decay channels increases dramatically with an increase of porphyrin array length.

In long **Z32** porphyrin arrays, the photobleaching in fluorescence intensity trajectories of 173 single porphyrin arrays exhibits complicated behaviors with large intensity fluctuations and multiple stepwise photobleaching behaviors. Thus, the recorded fluorescence intensity trajectories can be largely classified into two groups depending on the photobleaching behaviors (Supporting Information 3). Figure 3b shows the histogram of survival times for two groups in **Z32** porphyrin arrays. Single **Z32** arrays with stepwise photobleachings show relatively longer survival times as compared to those with large fluctuations (off-states) and complex photobleachings behaviors. This feature can be deduced because many off-states are

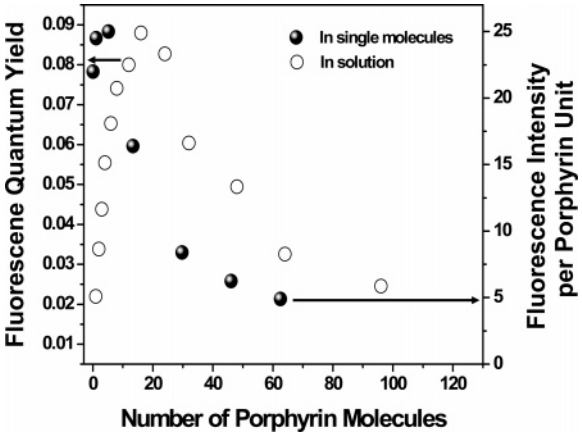

Figure 4. The plot of average values of fluorescence intensities for each porphyrin molecule in the array and the fluorescence quantum yields in solution versus the number of porphyrin molecules in the array.

nonradiative deactivation channels, indicating largely different conformations such as structural kinks in **Z48** porphyrin arrays, as shown in the highlighted STM image (Supporting Information 4). A clear image of single porphyrin array suggests conformational flexibility in longer arrays, which is reflected in fluorescence intensity trajectories. Therefore, we think that the off-process of several tens of milliseconds could arise from conformational heterogeneity.

For long arrays such as **Z32**, a sum of vibrational relaxation for linker sites between adjacent porphyrin molecules is a possible candidate for off-times. Another possible explanation for off-states is excitation energy transfer from the first excitation state to the triplet state or higher excitation state in a multiporphyrin array system. A simple calculation supports an explanation by energy transfer because excitation power of 1.5 μW at single molecule level leads to over two excitations per one porphyrin unit. The absorption cross section (σ) of **Z1** is calculated to be 7×10^{-16} cm^2 by extinction coefficient (ϵ), of 2.5×10^4 M^{-1} cm^{-1} at 543.5 nm. One photon of 543.5 nm light has an energy of 3.7×10^{-19} J. Thus, 1.5 μW average power at 543.5 nm corresponds to 4.0×10^{12} photons. Photon density in the diameter of focused beam spot (7.0×10^{-10} cm^2) has 5.7×10^{21} photons/cm^2. Also, the number of photons per absorption cross section of **Z1** porphyrin monomer is 4.0×10^6 photons. As a consequence, multiple excitations per one porphyrin unit are possible in the multiporphyrin array system.

In addition, the conformational heterogeneity in long porphyrin arrays can be confirmed at single molecule level by fluorescence intensity for each porphyrin molecule in the array. The initial fluorescence intensity of single porphyrin array in the fluorescence intensity trajectory divided by the number of porphyrin units in the array can be considered as the fluorescence intensity for each porphyrin molecule. The average values of fluorescence intensities for each porphyrin molecule in the array are compared to the fluorescence quantum yields of porphyrin arrays in solution as depicted in Figure 4.

The filled circles indicate the average values of fluorescence intensity distributions for each porphyrin molecule at single molecule level in **Z3**, **Z4**, **Z8**, **Z16**, **Z32**, **Z48**, and **Z64** porphyrin arrays. The open circles indicate the fluorescence quantum yields of porphyrin arrays (**Z1**−**Z96**) in solution. As seen in this plot, there is a mismatch in the maximum values between the two experimental data. This can be explained by a difference in the degree of freedom of porphyrin array molecules between solution and polymer matrix. Initial fluorescence intensities in fluorescence intensity trajectories are related to the fluorescence probability via absorption in single porphyrin arrays. Thus, the initial fluorescence intensity should increase in long arrays due to increased absorption cross-section values. However, as mentioned above, the fluorescence intensity for each porphyrin molecule (i.e., the initial fluorescence intensity divided by the number of porphyrin molecules in the array) in the **Z16**, **Z32**, **Z48**, and **Z64** arrays is lower than that of the **Z8** array, indicating that the number of fluorescence trap sites increases in longer arrays due to nonlinear structural heterogeneities as compared to relatively short arrays such as **Z8**.

Single Molecule Emission Spectra. The single molecule spectroscopic measurements of porphyrin arrays make it possible to observe the fluorescence behaviors of each porphyrin array contributed by nonradiative decay channels. The spectral distribution of each array provides more information on the nonradiative decay channels due to conformational heterogeneity.

Figure 5a shows the fluorescence spectra of single **Z8**, **Z16**, and **Z32** arrays, and their spectra were compared to the fluorescence spectra in solution. The spectra were recorded with an exposure time of 10 s. Thus, the spectra are actually a summation of fluorescence dynamics of a single array molecule for 10 s. The overall fluorescence spectral shapes of single **Z8**, **Z16**, and **Z32** porphyrin arrays are roughly similar to the fluorescence spectra in solution. However, the fine structures in the fluorescence spectra are different from those in solution. As reasons for various spectral shapes, we can think of the possibilities of aggregation of porphyrin arrays, which can be induced by a close contact or interaction between porphyrin arrays. Considering the concentration adopted in our single molecule fluorescence measurement and the collection of fluorescence spectra from each single array, the formation of aggregates responsible for the red-shifted spectral shapes can be eliminated. Thus, we think that various fluorescence spectral shapes arise from the difference in local environment and the structural difference of each array.

Interestingly, as the number of porphyrin units increases in the array from **Z8** to **Z32**, the emission spectra shift to low energy, resulting in a red-shifted distribution within the fluorescence spectral window in solution. Figure 5b shows the distribution of maximum fluorescence intensity values in the fluorescence spectra of single **Z8**, **Z16**, and **Z32** arrays. It can be seen that the emission maximum shifts to lower energy in the spectral distribution as the number of porphyrin molecules increases from **Z8** to **Z32**. There are two bands in the fine structures of fluorescence spectra of single porphyrin arrays. As seen in Figure 5a, for single **Z8**, **Z16**, and **Z32** arrays it is observed that the fluorescence maximum gradually shifts to low energies. This feature can be explained by that the energy variations of each constituent porphyrin moiety in the array become larger due to increased conformational heterogeneities as the array length increases. Thus, as the conformational heterogeneity becomes severe in longer porphyrin arrays, there is a large variation in energy among the constituent porphyrin moieties in the array due to a difference in local environment. Consequently, fluorescence occurs from the lowest energy porphyrin molecule in the array mediated by sequential energy

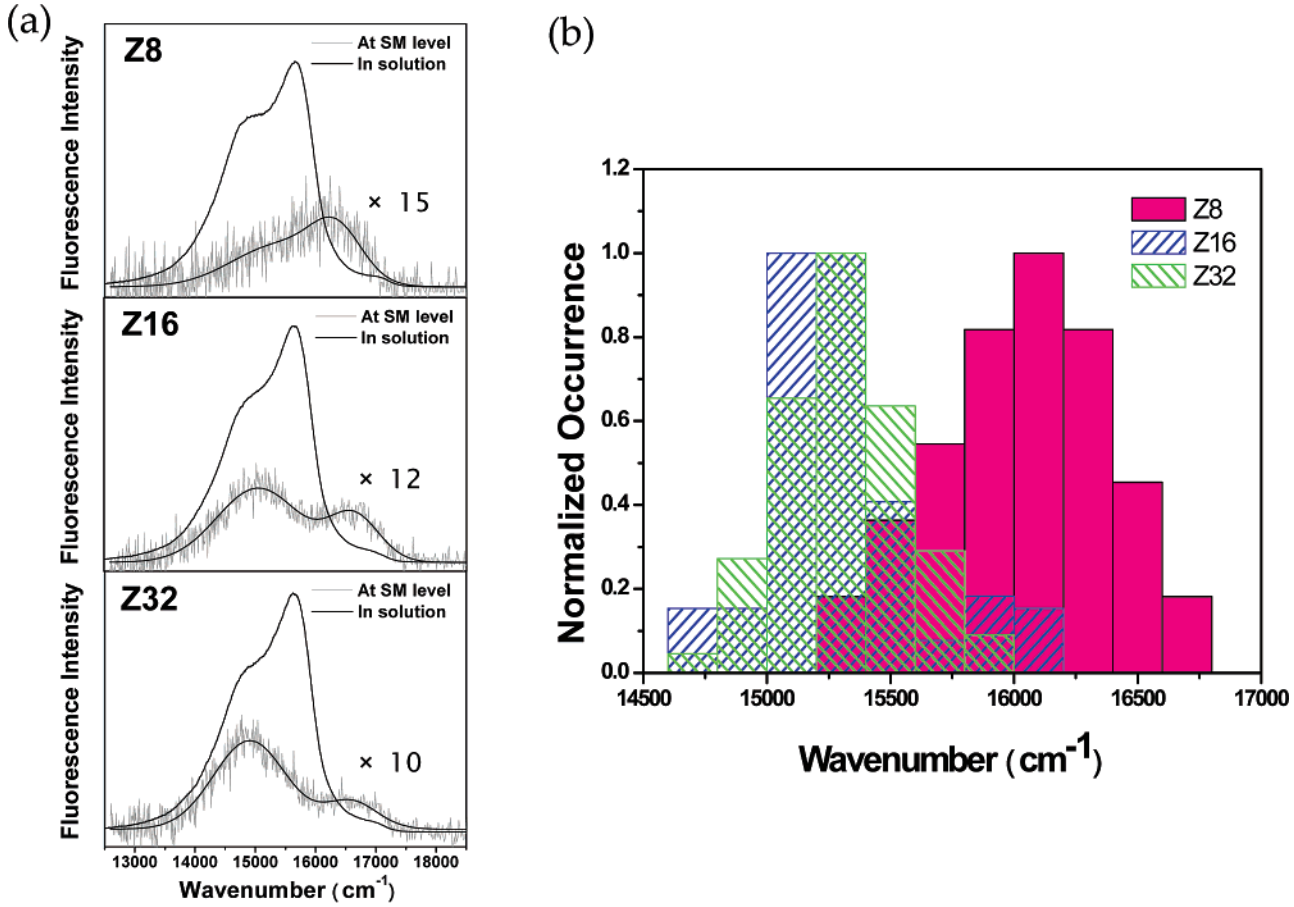

Figure 5. Representative of fluorescence spectra detected from single **Z8**, **Z16**, and **Z32** arrays by excitation at 543.5 nm (a). Distribution of fluorescence maximum positions recorded for **Z8**, **Z16**, and **Z32** in PMMA polymer matrix (b).

transfer processes.[26,27] This observation can also support the conformational heterogeneity existing in longer porphyrin arrays.

Conclusions

We have investigated the fluorescent properties of directly *meso*−*meso* linked porphyrin arrays (**Z*n***, ***n*** = **1**, **2**, **3**, **4**, **6**, **8**, **9**, **12**, **16**, **32**, **48**, **64**, and **96**) on single molecule level to seek for the possibilities of application as molecular photonic wires. The steady-state and time-resolved study of a series of porphyrin arrays in solution reveals the formation of conformational heterogeneities, which can provide nonradiative decay channels in longer arrays. To investigate the detailed fluorescence properties of porphyrin arrays, we have employed single molecule spectroscopic methods. The fluorescence intensity trajectories of **Z*n*** arrays show multiple stepwise photobleaching behaviors up to **Z8**. On the other hand, as the array becomes longer than **Z8**, the complicated photobleaching behaviors in fluorescence intensity trajectories, the decrease of initial fluorescence intensity level, and the spectral distributions of fluorescence spectra of single porphyrin arrays illustrated the existence of fluorescence traps due to the kink structures in longer porphyrin arrays. This result provides a clue to the number of porphyrin molecules maintaining a well-defined linear structure in the directly linked orthogonal porphyrin arrays. Our study also will be useful in devising single molecule devices based on porphyrin arrays especially for applications as molecular photonic wires.

Acknowledgment. This research was financially supported by the National Creative Research Initiatives Program of the Korea Science and Engineering Foundation of Korea (D.K.). The work at Kyoto was supported by CREST (Core Research for Evolutional Science and Technology) of Japan Science and Technology Corp. (JST). We thank Dr. N. W. Song at Korea Research Institute of Standards & Science and Dr. N. K. Lee at Seoul National University for helpful discussions.

Supporting Information Available: Fluorescence images of **Z8** embedded in a PMMA polymer matrix at atmospheric condition, steady-state absorption and fluorescence spectra of **Z1**−**Z48** porphyrin arrays in THF, fluorescence intensity trajectories of **Z32**, and STM images of **Z6**, **Z9**, and **Z48**. This material is available free of charge via the Internet at http://pubs.acs.org.

JA0544861

(26) Vosch, T.; Hofkens, J.; Cotlet, M.; Köhn, F.; Fujiwara, H.; Gronheid, R.; Van Der Biest, K.; Weil, T.; Herrmann, A.; Müllen, K.; Mukamel, S.; Van der Auweraer, M.; De Schryver, F. C. *Angew. Chem., Int. Ed.* **2001**, *40*, 4643.
(27) Vosch, T.; Cotlet, M.; Hofkens, J.; Van Der Biest, K.; Lor, M.; Weston, K.; Tinnefeld, P.; Sauer, M.; Latterini, L.; Müllen, K.; De Schryver, F. C. *J. Phys. Chem.* **2003**, *107*, 6920.
(28) Gronheid, R.; Hofkens, J.; Köhn, F.; Weil, T.; Reuther, E.; Müllen, K.; De Schryver, F. C. *J. Am. Chem.* Soc. **2002**, *124*, 2418.
(29) Ying, L.; Xie, X. S. *J. Phys. Chem. B* **1998**, *102*, 10399.
(30) Liu, R.; Holmanm, M. W.; Zang, L.; Adams, D. M. *J. Phys. Chem. A* **2003**, *107*, 522.
(31) Hernando, J.; Van der Schaaf, M.; Van Dijk, E. M. H. P.; Sauer, M.; Garæia-Parajó, M. F.; Van Hulst, N. F. *J. Phys. Chem. B* **2003**, *107*, 43.